Higher Harmonic Ultrasonic Guided Waves for Structural Integrity Assessment of Dry Storage Canisters – 15381

Gloria Choi*, Yang Liu, Cliff Lissenden**
Department of Engineering Science and Mechanics, The Pennsylvania State University, University Park 16802
* gwc5041@psu.edu;**lissenden@psu.edu

ABSTRACT

Dry storage of used fuel from nuclear power plants has gone from an interim storage solution to a longer-term solution, which necessitates monitoring the integrity of the stainless steel canister that confines the used fuel. Since the storage facilities are located around the country in a variety of different environments there is a wide range of degradation mechanisms that could occur over time in the cylindrical canister. One potential degradation mode that has created significant concern is stress corrosion cracking. We propose using higher harmonic ultrasonic guided waves as a tool to nondestructively inspect used fuel canisters. Higher harmonics are generated when a wave propagates through a nonlinear elastic media. These higher harmonics have been shown to be quite sensitive to microstructural features such as dislocation substructures, persistent slip bands, precipitates, etc. The use of ultrasonic guided waves to inspect the canister is attractive due to the size of the canister and the ability of guided waves to inspect a reasonably large domain relative to traditional bulk wave ultrasonics. We will highlight our recent progress on theory, numerical simulations, and laboratory experiments to develop higher harmonic guided waves as a tool to detect microstructural changes that precede macroscale damage. Analyzed structures include plates and hollow cylinders, and we focus on localized damage initiation, as is the case for stress corrosion cracking.

Recent experiments focus on using magnetostrictive transducers in activating the fundamental shear horizontal mode (SH0) and the third harmonic that is generated due to the material nonlinearity. The magnetostrictive transducer comprises a thin iron-cobalt foil, a meandering electric coil, and a permanent magnet. These transducers are inexpensive, easy to use, and are very efficient at generating shear waves. In applications where the wavelength is larger than the plate thickness, the waves are guided by the traction free boundary conditions and propagate in the plane of the plate. For this canister application, the shear horizontal waves energize the entire thickness of the canister and propagate along the shell in the direction dictated by the meander coil. Experiments indicate that magnetostrictive transducers can generate waves that propagate in plate thicknesses of 1 mm to at least 16 mm. The SH0 mode is nondispersive and generates a third harmonic of the same mode that is shown to be sensitive to localized plastic strain and unseen fatigue damage. It has a strong potential to detect the very early stages of stress corrosion cracking. Due to the geometric configuration of dry storage casks, the transducers will need to be delivered to the inspection points by a robotic system that navigates through the cask ventilation system.

INTRODUCTION

With the increased use of extended dry storage systems for longer term storage and handling of commercially spent or used nuclear fuel, there is a need to monitor the structural integrity of the components due to the possible damages associated with certain environment conditions and extended periods of storage. Stainless steel canisters, which encase the fuel rods (i.e zirconium alloy cladded tubing containing uranium dioxide pellets), can be susceptible to chloride-induced stress corrosion cracking (SCC) depending on alloying compositions and the atmospheric environmental conditions (i.e. near coastal areas), since several dry storage systems utilize passive ventilation that allow for interaction of moist air with the metal surface. [1, 2] Hence, content of such moist air in some environments can contain various salts such as chloride, nitrate and sulfate salts. In addition, only for a long storage duration (couple of hundreds of years) is pitting/crevice corrosion of concern for canister integrity. [1]

The history of dry storage system conditions and the specific fuel would determine the current temperature and rate of temperature drop. The following are some thermal release behaviors specific to particular dry storage systems, which provide approximate temperature range required of operation of possible transducers for inspection. With known cask heat transfer codes and decay heats of ORIGEN, cladding temperature was computed to decrease from 380°C to 100°C between years 5 and 15 of cooling with 30 GWD/MtU burnup, but stay constant about 100°C for the following 90 years. [3] Similarly, as for the conditions with investigations conducted by Peehs et al on Ziracloy cladding, temperatures can be above 300°C for the first two years in dry storage but exhibit rapid decrease. The following phases after this initial period continues with slower rates of temperature drop after 300°C. Eventually, temperature drops are negligible once it has reached below 120C. [4-6] In addition, simulation studies involving blocked ventilation of a Holtec HI-STORM 100 had estimated centerline temperature profile between 200-500°C, while normal operating temperature conditions were calculated to be between 100-300°C. [7]. Hence, at least the latter years of the used nuclear fuel, inspection devices should be designed to be operable up to 300°C.

Both traditional bulk wave and guided wave ultrasonic techniques have the potential to nondestructively evaluate damages that can be present with dry cask storage of used nuclear fuel. Guided waves propagate along a boundary and can be used for inspection of longer distances than bulk waves, but as multiple modes can be excited, consideration must be placed into proper mode selection and excitation design. Magnetostrictive transducers have the advantage of being couplant-free and some can be operable during temperature ranges of dry cask storages. Studies of Kawahara et al [8] report the Curie temperature (where demagnetization occurs) to be 1097°C for 50-50 Fe-Co alloys and indicate the maximum saturation magnetization occurs at room temperature. With higher operation temperatures the saturation magnetization gradually decreases, such that at 987°C, the saturation magnetization has decreased to 70% of maximum value. High temperature ceramic/graphite adhesives can be used for bonding the thin layer magnetostrictive foil on non-ferromagnetic metals. Experiments indicate that magnetostrictive transducers can generate waves that propagate in plate thicknesses of 1 mm to at least 16 mm, and thicknesses of stainless steel canister of some dry storage design fall within this range (i.e. The Hi-StORM100 with 12.7 mm (0.5 in)). [1]. Magnetostrictive transduction is complete with the addition of a permanent magnet, some are capable of retaining a magnetic field at high temperatures, and the alternating current provided by a meander coil. These transducers behave as sensors such that the alternative current direction parallel to applied magnetic field (from permanent magnet) and alternating displacements are produced due to changes in magnetic domains. The reciprocal effect is also used to receive a propagated shear wave.

The intended approach is directed towards inspection of the metal canister of the dry cask design and focus on capability of tracking age-related degradation, corrosion, and other microstructural changes. There are a limited number of works in characterizing SCC via ultrasonics in pipe and plate-like structures, but they demonstrate how ultrasonic waves have been sensitive to SCC and there is potential for structural health monitoring dry storage metal containers. Spanner & Selby [9] developed a nondestructive technique with the ability to measure SCC depth for pipelines. Zumpano and Meo conducted a simulation study for using nonlinear elastic time reversal acoustic method for locating and characterizing SCC in welded plate-like structures [10]. Baby et al [11] demonstrated ultrasonic creeping wave transducers were able to detect inner diameter cracks due to SCC of X-20 pipes. We have conducted some preliminary experimental and simulation studies in using magnetostrictive transducers to characterize localized deformation within a medium via nonlinear guided wave phenomenon. The cumulative nature of specific primary-higher harmonic mode pairs was verified and deviation from normalized modal amplitude ratio trend demonstrated the influence of localized plastic deformation. Further investigation can be done for the application of nonlinear guided wave inspection of the metallic canisters via magnetostrictive transducers.

The basis of nonlinear ultrasound is the phenomenon where a sinusoidal ultrasonic generates higher harmonics as the wave interacts with the microstructure. Nonlinearity contributions include crystalline lattice anharmonicity, dislocations and other microstructure features. Evidently, progressive damage is expected to occur from microscale and eventually project to macroscale changes, hence changes the degree of nonlinearity can be due to material damage contributions. Differentiating material contributions from system contributions must be resolved. Our recent work has demonstrated that the fundamental shear horizontal mode is sensitive to progressive localized damage associated with microscale changes that are present prior to visible macroscale deformation. We propose to use higher harmonic ultrasonic guided waves to nondestructively locate and characterize damage like SCC in used fuel canisters during the use of the dry storage system. SCC typically involves external surfaces where chlorides have been deposited, with large dependence on induced stress, temperature, pH, and chloride ion concentration dependence. [12] Precursors of chloride-induced stress-corrosion cracks are pitting, where once a critical size is reached crack propagation occurs. [13] These features (changes in lattice anharmonicity and crack growth) are both sources of material nonlinearity [14], that could be characterized and monitored via higher harmonic ultrasonic guided waves.

DESCRIPTION AND DISCUSSION OF PRIOR WORK

Extensive theoretical work and experimental verification was done by Liu et al [15] to identify the specific modes that generate higher harmonics that are cumulative with propagation distance, which meets two the internal resonance conditions of (1) phase speed matching between primary and secondary modes and (2) non-zero power flux transfer from the primary to secondary mode. With known cumulative trends with propagation distance for undeformed material state, the material nonlinearity changes have the potential to result in deviation from this trend. The fundamental shear horizontal mode (SH0) has been selected in our analysis. The intent of this paper is to provide a review of previous work where our focus has been on exciting fundamental shear horizontal through various damaged specimens and investigate the third harmonic response. Prior theoretical analysis indicates that particular modes, which satisfy the two criteria can generate cumulative higher harmonics, should be advantageous for longer distance inspection. Our recent progress includes numerical simulations and laboratory experiments in utilizing higher harmonics to detect microstructural changes associated with localized damage before macroscale damage is present.

The synthesizer of the RITEC RAM-5000 Snap system generates the signal, which goes through the built-in high power gated amplifier. The signal proceeds to travel through a 50 Ohm load, a matching network, then the transmitting transducer. The cumulative study of the third harmonic used a shear transducer to receive the propagating wave, which is observed and acquired via an oscilloscope. The other two experiment sets of monotonically loaded and cyclically loaded specimens had a receiving magnetostrictive transducer configuration and additional matching networks that replaced the shear transducer.

Cumulative Third Harmonic in Untested Plate

We have experimentally verified the cumulative nature of the third harmonic in a pristine untested specimen, 914.4 mm x 914.4 mm aluminum 2024-T3 plate with thickness of 1 mm, which is briefly described in Lissenden et al [16] with further details provided in the following text. This setup involved exciting a 10 cycle f_0=0.80 MHz toneburst signal via a magnetostrictive transducer with meander coil wavelength (λ) of 3.6 mm and receiving the wave via shear transducer with central frequency of 2.25 MHz with syrup as the couplant, as shown in Figure 1. The shear transducer was selected as the receiver to allow for multiple measurements at several propagation lengths progressively further from the transmitter. In addition, a fixture was used to minimize couplant effect where pressure on the shear transducer could be controlled based on number of turns on a lever. The primary excitation was a 10-cycle fundamental shear horizontal mode at 0.80 MHz. Time domain signals were acquired with eight repetitive measurements obtained for each location at increments of 10.6λ between 42.3λ to 148.2λ from the transmitter.

A sample time domain signal is shown in Figure 2. The wave packet encased by dashed rectangle is the SH0 wave packet, following packets are due to wave interactions with the finite size of the magnetostrictive foil edge. Via Matlab, the SH0 wave packet was analyzed using a Tukey window and the amplitudes of both the primary mode and third harmonic were tracked from the frequency spectrum. The upper two plots of Figure 3 show the resulting frequency signal indicating similar primary mode SH0 amplitudes for propagation distances 42.3λ and 84.7λ, with notable 3rd harmonic amplitude (lower two plots) increase after doubling the propagation distance. Modal amplitude ratios were averaged from the eight measurements at each location, and normalized with respect to the averaged value (0.01526) at 42.3λ and shown in Figure 4.

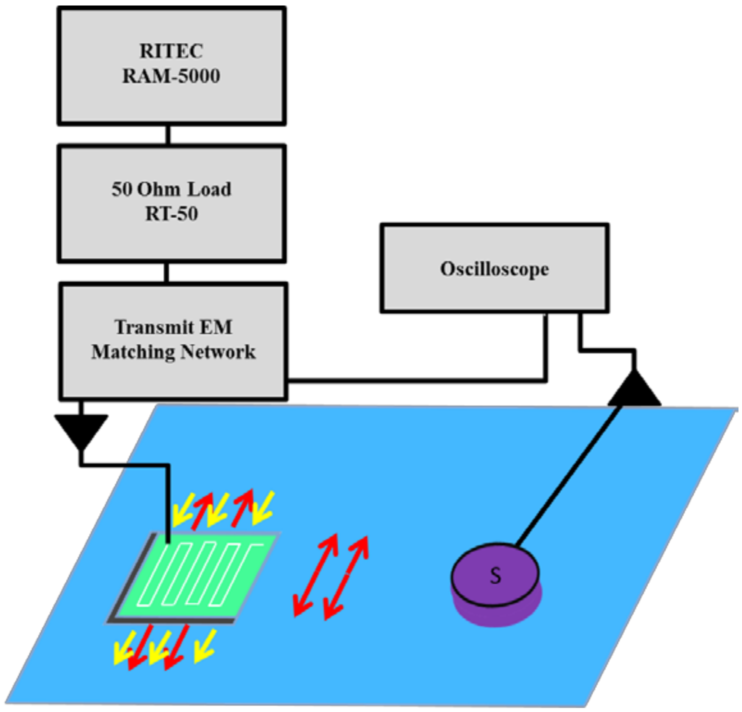

Fig. 1. Schematic of experimental test setup for investigating SH0/sh0 primary/third harmonic trend.

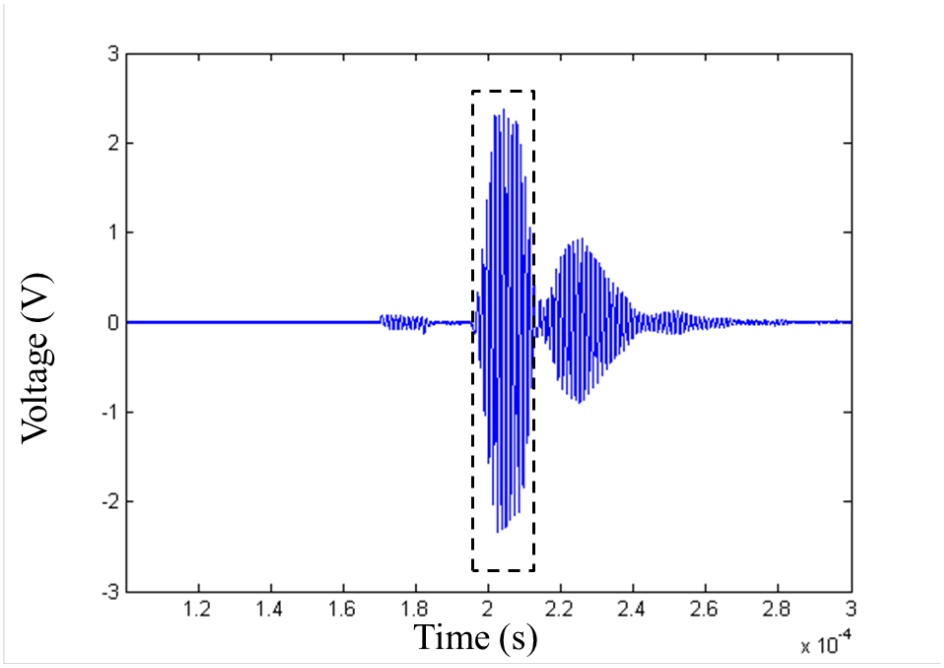

Fig. 2. Time domain signal received at 42.3λ from the transmitter.

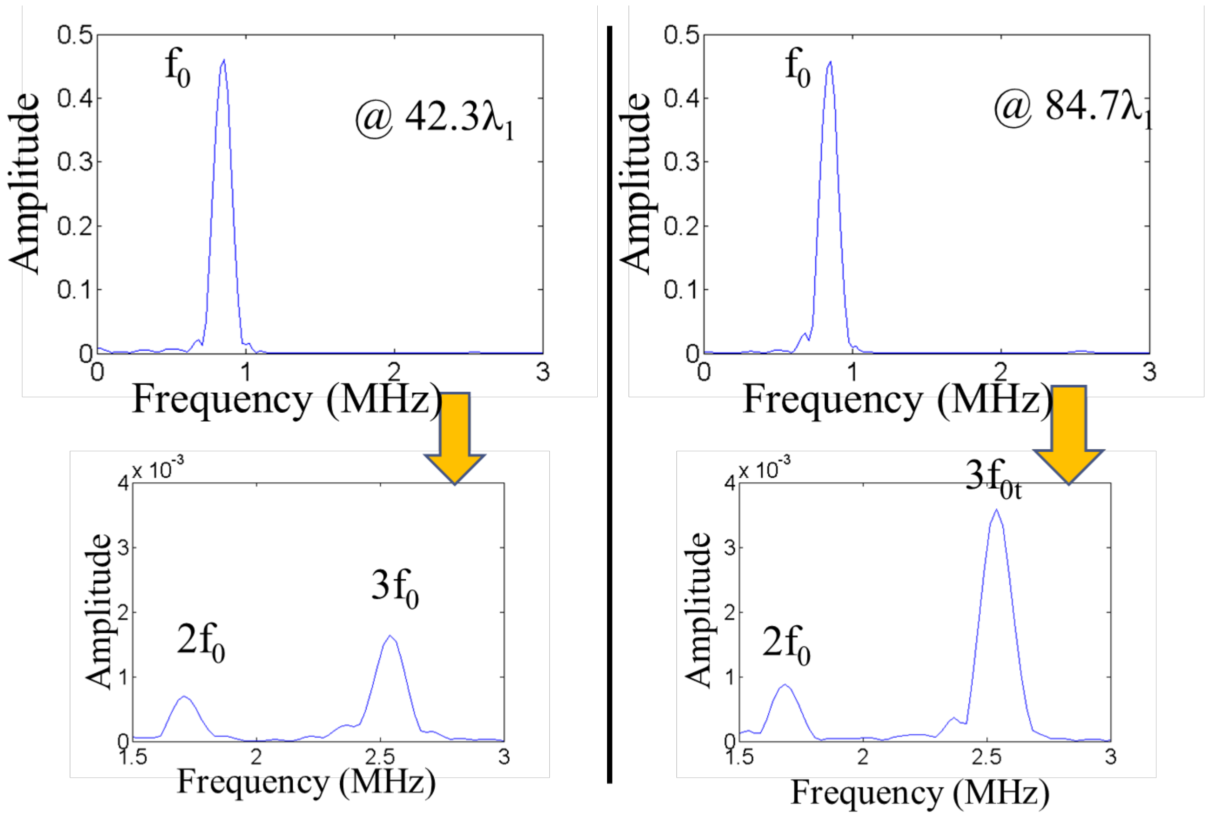

Fig. 3. Frequency spectra of SH0 after propagation distances of 42.3λ and 84.7λ, where the lower two plots shows zoom-in scale of second/third harmonic response.

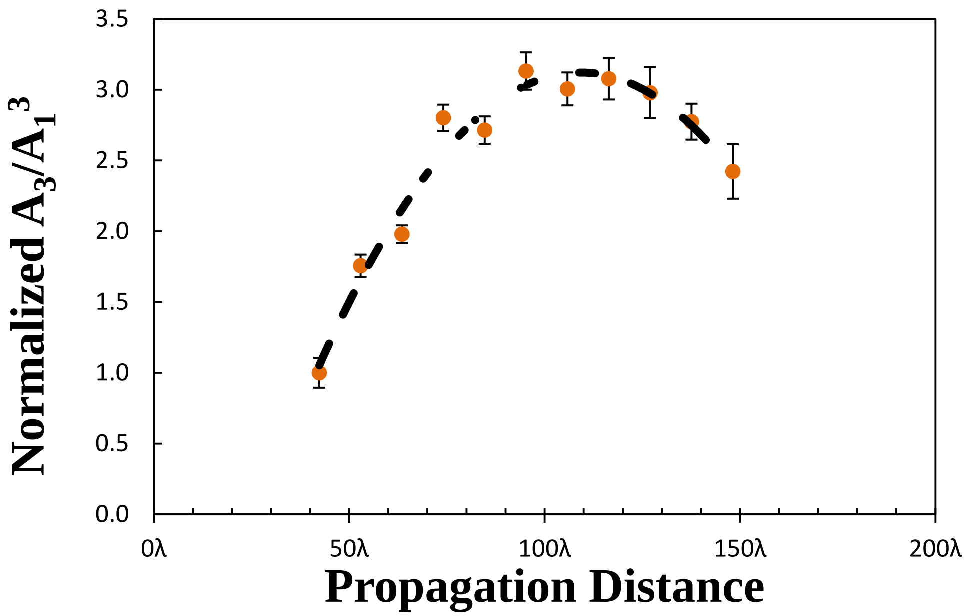

Fig. 4. Modal amplitude ratio of third harmonic to primary mode cubed as a function of propagation distance and normalized with respect to 0.01526. [16]

Standard error and quadratic regression line are included within the plot. For some distance, the modal amplitude increases and then decreases. During the initial increasing trend, the predicted phase matching and power flux transfer between primary to third harmonic are dominant. The decreasing trend with further propagation distance is due to diffraction effects, which are often not included in simple modeling efforts.

Third Harmonic and Monotonically Loaded Plates

Aluminum thin strips were plastically deformed with monotonic tensile loading, where further details can be found in Lissenden et al [17]. Original notched lengths are indicated as the number following the “DEF-“ in inches. Transmitter and receiver magnetostrictive transducers had meander coil wavelengths respectively of 3.6 and 1.2 mm, along with the setup shown in Figure 5. Analysis on the received SH0 (f_0=0.83 MHz 15 cycle) on six different specimens revealed general dependence of notch length percentage of propagation distance on normalized modal amplitude ratio A_3/A_1^3, where circular markers are averaged values of ten replicate measurements along with standard error in Figure 6. Sample DEF-18, DEF-9, and DEF-4 have been interrupted such that the maximum plastic strain (MPS) were similar values falling between 6.5-7.4%. Sample DEF-2 had to be stopped at a lower value where the MPS was 4.7%, so fracture would not occur and the specimen would be intact for third harmonic investigation. It is evident how the length of the localized damage with respect to the SH0 mode propagation distance influences the A_3/A_1^3 ratio. Higher notch length percentage of propagation distances than 20% resulted in higher A_3/A_1^3 ratios. For sample DEF-18, the transducers were placed within the notched length, presented as 100% notch length percentage of propagation distance, and notably exhibited approximately 5 times higher A_3/A_1^3 than the ratio of undeformed DEF-0. Pruell et al has similar results using the S1 Lamb mode with an angle beam transducer at 2.225 MHz and analyzed the receiving S2 Lamb mode second harmonic through 1100-H14 aluminum plates with progressive plastic deformation. They reported an increase by a factor of 2 in the harmonic amplitude ratio A_2/A_1^2 between their as-received and plastically deformed (1.7%) sample. [18].

Sensitivity of the SH0 mode to damage severity is demonstrated by these two samples with the same original notch length of 228.6 mm, but the two were deformed such that the MPS was 6.8 and 8.4%. The A_3/A_1^3 ratio is slightly higher for the further plastically deformed specimen and both comparably higher than the dashed line indicating the A_3/A_1^3 value from DEF-0, as shown in Figure 7. While sensitivity of SH0/sh0 primary/third harmonic mode to progressive and localized damage has been briefly considered with these experiments, work is in progress to determine correlation between microstructural changes to nonlinear ultrasonic guided waves via theoretical modeling.

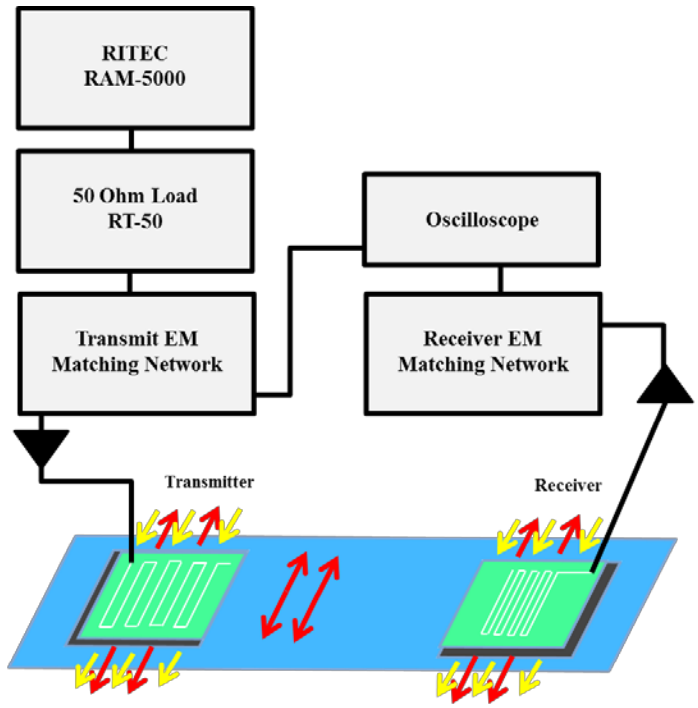

Fig. 5. Schematic of experimental test setup for investigating SH0/sh0 primary/third harmonic trend in deformed plates. Meander coils for transmitter and receiver configuration respectively have wavelengths of 3.6 and 1.2 mm.

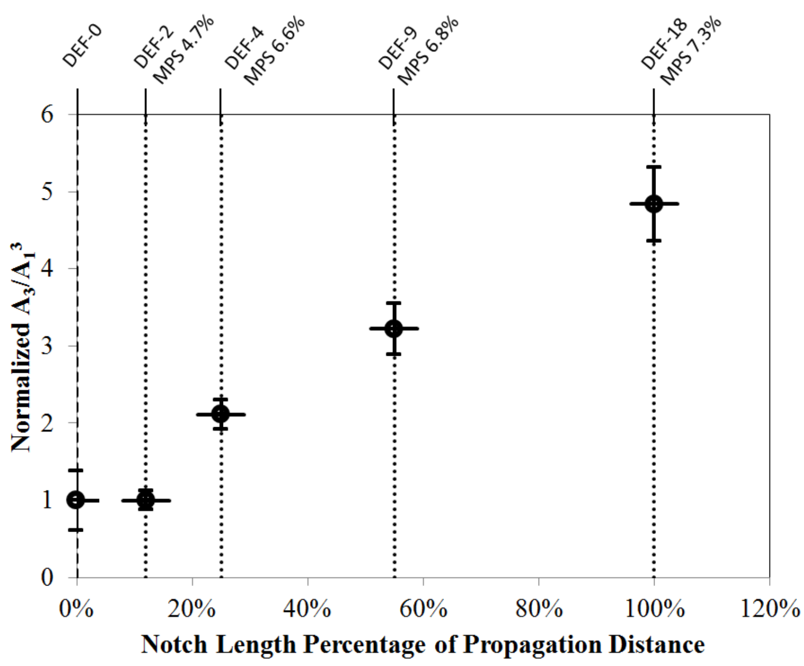

Fig. 6. Normalized modal amplitude ratios as a function of the notched region that was within the propagation distance (430 mm), where values were normalized to the average value for sample DEF-0 with value 0.1395. [19]

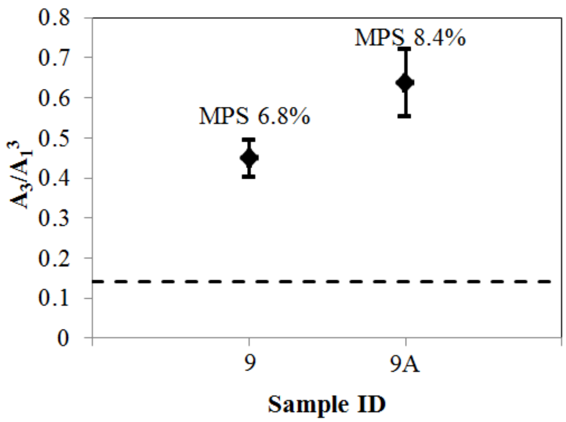

Fig. 7. Modal amplitude ratios for two samples with different MPS values for original notch length of 228.6mm for SH0 propagation distance of 430 mm, dashed line indicates A_3/A_1^3 for DEF-0. [19].

In addition, another group of aluminum plates were cyclically loaded with full experimental details provided by Lissenden et al [16]. One plate was first cyclically loaded to failure, which was found to be 4,539 cycles. Four additional specimens were cycled up to 20, 40, 60, and 80% of the fatigue life of this first plate, with no visible cracks. After the surface was cleaned with acetone and magnetostrictive foils were bonded 240 mm apart, 15-cycle tone bursts with central frequency 0.83 MHz were excited through each of these specimens and an untested specimen. The experimental setup shown in Figure 5 was used. Results are shown in Figure 8 where average values of 10 replicate measurements for each sample are plotted along with standard error as a function of fatigue life. With progressive fatigue damage, the mean value increases progressively and could be fitted with a third degree polynomial regression line, where the A_3/A_1^3 ratio increases with fatigue cycling.

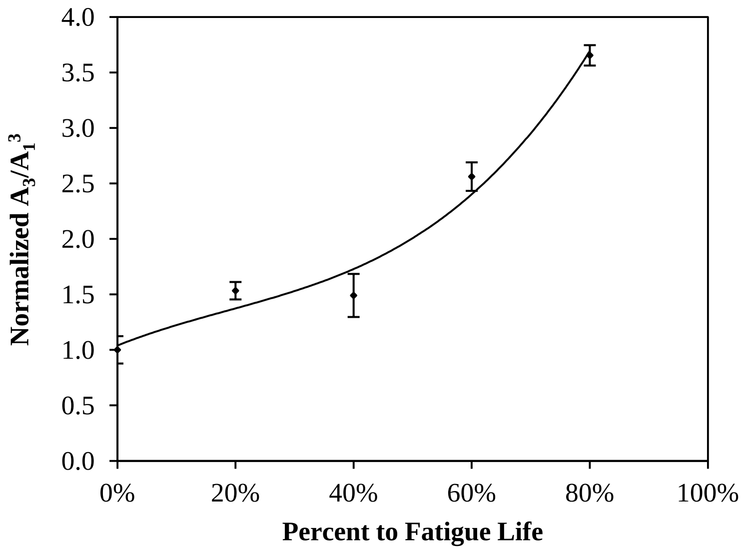

Fig. 8. Modal amplitude A_3/A_1^3 for five different fatigue specimens. [16]

CONCLUSIONS

Our previous work involving the fundamental shear horizontal SH0/sh0 primary and third harmonic mode pair have been summarized and has provided us with confidence that nonlinear guided waves are sensitive to microstructure changes associated with monotonic tensile plastic deformation and cyclic loading. Further work is in progress in considering theoretical modeling the relation between the related microstructure changes (material nonlinearity changes) with the interaction of nonlinear guided waves for characterization purposes. Our approach can also be applied to detect the very early stages of stress corrosion cracking of stainless steel canisters of dry storage.

ACKNOWLEDGEMENTS

These presented materials are based upon work supported by the Nuclear Energy Universities Program number award number DE-NE0008266.

REFERENCES

1. D.B. Rigby. *Evaluation of Technical Basis for Extended Dry Storage and Transportation of Used Nuclear Fuel*; December 2010. Prepared for U.S. Nuclear Waste Technical Review Board.
2. ASTM C 1562 – 10, "Standard Guide for Evaluation of Materials Used in Extended Service of Interim Spent Nuclear Fuel Dry Storage Systems," ASTM International, pp. 1-24.
3. M. E. Cunningham, E. P. Simonen, R.T. Allemann, I. S. Levy, I. S., R.F. Hazelton, and E. R. Gilbert, *Control of Degradation of Spent LWR Fuel During Dry Storage in an Inert Atmosphere*, PNL-6364, Pacific Northwest Laboratory, Richland, WA, 1987.
4. M. Peehs and K. Einfeld, *Effects of Long Term Dry Storage of Spent Nuclear Fuel*, HLRWM Conf., Las Vegas, NV, April 1992.
5. M. Peehs, M., and Banck, Y., *Spent Fuel Storage-A Reliable Technology in the Back-end of the Fuel Cycle*, Proc. 1993 Intl, Conf. On Nuclear Waste Management and Environmental Remediation, Prague, 1993.
6. Peehs, Martin, Garzarolli, and Goll, W., *Assessment of Dry Storage Performance of Spent LWR Fuel Assemblies with Increasing Burn-Up, Intl. Symposium on Storage of Spent Fuel from Power Reactors*, Vienna, Austria, Nov. 9-13, 1998.
7. A. Malliakos. *A Pilot Probabilistic Risk Assessment of a Dry Cask Storage System at a Nuclear Power Plant*, U.S. Nuclear Regulatory Commission, NUREG-1864, March 2007.
8. K. Kawahara, D. Iemura, S. Tsurekawa and T.Watanabe. *High Temperature In-situ Observations of Magnetic Domains in Fe-Co Alloys*. Materials Transactions, Vol. 44, No. 12 (3002) pp. 2570-2577.
9. J. Spanner and G. Selby. *Sizing Stress Corrosion Cracking in Natural Gas Pipelines Using Phased Array Ultrasound.* ASME 2002 pressure vessels and piping conference. Vancouver, Canada 2002
10. G. Zumpano, M. Meo. *A new nonlinear elastic time reversal acoustic method for the identification and localization of stress corrosion cracking in welded plate-like*

structures-a simulation study. International journal of solids and structures. Volume 44, Issues 11-12, June 2007, pages 3666-3684.

11. S. Baby, T. Balasubramanian, R.J. Pardikar. *Ultrasonic Study for Detection of Inner Diameter Cracking in Pipeline Girth Welds using Creeping Waves*. International Journal of Pressure Vessels and Piping. Volume 80, Issue 2, February 2003, pages 139-146.
12. S. Ghosh, V. Kain. *Effect of Surface Machining and cold working on the ambient temperature chloride stress corrosion cracking susceptibility of AISI 304L stainless steel*. Materials Science and Engineering: A. Volume 527, Issue 3, 15 January 2010, Pages 679-683
13. D.T. Spencer, M.R. Edwards, M.R. Wenman, C. Tsitsios, G.G. Scatigno, P.R. Chard-Tuckey. The initiation and propagation of chloride-induced- transgranular stress-corrosion cracking (TGSCC) of 304L austenitic stainless steel under atmospheric conditions.
14. J. H. Cantrell, W. T. Yost. Acoustic nonlinearity and cumulative plastic shear strain in cyclically loaded metals. Journal of Applied Physics 113, 153506 (2013)
15. Y. Liu, V. K. Chillara, C. J. Lissenden, and J. L. Rose. *Third harmonic shear horizontal and Rayleigh lamb wave in weakly nonlinear plates.* Journal of applied physics 114, 114908 (2013).
16. C. Lissenden, Y. Liu, V. K. Chillara, G. Choi, X. Yao. *Nonlinear guided waves for continuous material microstructure state awareness*. Proceedings of the ASME 2014 International Mechanical Engineering Congress and Exhibition IMECE 2014-39699. November 14-20, 2014 Montreal, Canada. (In process)
17. C. J. Lissenden, Y. Liu, G. W. Choi, X. Yao. *Effect of localized Microstructure on Higher Harmonic Generation of Guided Waves.*Journal of Nondestructive Evaluation (2014) 33: 178-186.
18. C. Pruell, J. Y. Kim, , J. Qu, L. J. Jacobs: A nonlinear-guided wave technique for evaluating plasticity-driven material damage in a metal plate. NDT&E Int. **42**, 199–203 (2009)
19. G. Choi, Y. Liu, C. J. Lissenden, J. L. Rose. *Influence of localized microstructure evolution on second harmonic generation of guided waves*. In: Thompson, D.O., Chimenti, D.E. (ed) Review of Progress in Quantitative Nondestructive Evaluation (2014, in progress)